frontiers | Frontiers in Earth Science

ORIGINAL RESEARCH
published: 30 June 2022
doi: 10.3389/feart.2022.862710

Adaptability Analysis of Full Height Mining at One Time of Deep Soft Thick Coal Seam

Qinghai Li[1], Haonan Wang[1], Xuejun Zheng[2], Kaixin Li[3], Yonghu Ji[2] and Zijun Wang[1]*

[1]College of Energy and Mining Engineering, Shandong University of Science and Technology, Qingdao, China, [2]Shandong Lilou Coal Industry Co., Ltd., Heze, China, [3]College of Geodesy and Geomatics, Shandong University of Science and Technology, Qingdao, China

With the improvement of technology and equipment, it is preferred to adopt full-height mining at one time when conditions permit. According to the specific geological conditions of no. 3 coal seam in Lilou Coal Industry, the feasibility of full-height mining and top-caving mining method for soft thick coal seam with large buried depth is analyzed by means of theoretical analysis, numerical simulation and field application analysis, which provides basis for the subsequent improvement of field mining method. Through the establishment of cantilever beam mechanical model of basic roof, the influence of two mining methods on the energy response of basic roof is analyzed. Based on the energy storage characteristics of coal seam, roof and floor measured in the field, the intensity of energy released from disturbed strata by two coal mining methods is analyzed. PFC2D numerical simulation was used to compare the roof failure of the two mining methods, to monitor the change of the stress in the coal seam after excavation, and to calculate the coal seam burial depth suitable for a full mining height by adjusting the *in-situ* stress. The results show that compared with top-coal mining, the elastic strain energy accumulated in the full-height roof beam is more, and the energy release intensity of disturbed rock is greater. The roof crack extension height is 9.1 m and the coal wall failure depth is 5.46 m under the condition of full mining height at one time. The roof crack extension height is 1.19 m and the coal wall failure depth is 2.19 m under the caving coal mining method. In the caving coal mining method, the stress level of the original rock is restored at 3 m in front of the coal wall, and the stress level of the original rock is restored at 5 m in front of the coal wall when the full mining height is once taken. It is safer to adopt full-height mining method when the buried depth of coal seam is less than 380 m. The research results can provide reference for mining soft thick coal seam with large buried depth.

Keywords: full height mining at one time, top caving mining, cantilever beam model, elastic strain energy, coal wall stability

OPEN ACCESS

Edited by:
Yuwei Li,
Liaoning University, China

Reviewed by:
Tong Zhao,
Taiyuan University of Technology, China
Meng Li,
China University of Mining and Technology, China

****Correspondence:***
Qinghai Li
liqinghai@sdust.edu.cn

Specialty section:
This article was submitted to Economic Geology, a section of the journal Frontiers in Earth Science

Received: *26 January 2022*
Accepted: *18 May 2022*
Published: *30 June 2022*

Citation:
Li Q, Wang H, Zheng X, Li K, Ji Y and Wang Z (2022) Adaptability Analysis of Full Height Mining at One Time of Deep Soft Thick Coal Seam. Front. Earth Sci. 10:862710. doi: 10.3389/feart.2022.862710

1 INTRODUCTION

China is rich in coal resources, and thick coal seam resources account for about 44.8% of the total coal reserves in China. The annual output of thick coal seam accounts for 40 ~ 50% of the national coal output, which provides energy guarantee for China's economic development. At present, there are three main methods for thick coal seam mining: slicing mining, full height mining at one time

and top coal caving mining. Slicing mining has some shortcomings, such as complex technology, low efficiency and poor economic benefits. At present, it has been basically eliminated in domestic mines, but the full height mining at one time process and mining equipment are relatively mature, which has been widely popularized and applied in China, and the mining height has increased from the earliest 4.5 m to over 8.0 m. Typical intelligent fully mechanized mining face with over 8.0 m mining height in Shangwan Coal Mine of Shendong Coal Group has been successfully put into operation (Wang et al., 2021; He et al., 2021; Zhang, 2020). Top coal caving mining method has strong adaptability to coal seam occurrence conditions, and has the advantages of full thickness mining at one time, high production efficiency, high economic benefits, etc. However, for hard roof, the rock strata integrity is strong and it is not easy to fall, and the coal recovery rate is low, so auxiliary measures such as hydraulic fracturing technology and loose blasting can be used to enhance caving property of top coal, and now caving property of top coal mining method is also widely used (Hubbret and Wills, 1957; Wong et al., 2002; Zhang et al., 2010; Wang and Pang 2018).

Although the theoretical mining height of top coal caving mining is the same as that of full height mining at one time, the working procedure of top coal caving mining is different from that of full height mining at one time, and there are some differences in the influence of the two methods on the stability of the working face (Kong et al., 2019; Hu et al., 2018; Zhang et al., 2016). In recent years, scholars at home and abroad have done a lot of research on the failure mechanism of the working face with full height mining at one time: Hu and Jin (2006) summarized the law and characteristics of rock pressure behavior in full height mining at one time stope by analyzing the field rock pressure data of the working face. Ning (2009) established a compression bar model with one end rigidly fixed and one end elastically fixed, and obtained the failure mechanism of coal wall in full height mining at one time working face. Gong and Jin (2008) established the mechanical model of roof with full height mining at one time according to the mechanical characteristics of rock structural plane, and put forward the control mechanism of roof conditions in different rock strata. Hao et al. (2004) obtained the interaction mechanism between overlying rock movement and support in full height mining at one time stope by studying the equilibrium structure of overlying rock mass. Xu et al. (Xu and Ju 2011; Liang et al., 2017) found in the research that when the mining height is increased, the fracture form of the first key layer above the coal seam changes from "masonry beam" structure to "cantilever beam" structure, and it is easy to collapse suddenly to the goaf. Under the conditions of "three soft", thick alluvium and extra-thick hard coal seam, the "cantilever beam" model of roof provides theoretical basis for the stability control of coal wall and roof in full height mining at one time working face (Liang et al., 2019; Zhang et al., 2020). At the same time, Ju et al. (2013, 2014, 2012) found that the collapse form of "cantilever beam" structure of roof strata would increase the periodic weighting interval of the working face through similar simulation experiments, field measurement and theoretical analysis. Yang et al. (2020) found through similar simulation and numerical analysis that the increase of suspended ceiling area will lead to the increase of cohesive energy of roof, and cohesive energy of roof is the main reason for the failure of coal and rock mass. Feng et al. (2019) combined theoretical analysis with on-site monitoring, and revealed the response mechanism of mining speed to the energy release from roof rock breaking, and found that the energy released from hard roof breaking was positively correlated with mining speed.

At present, the technology of full height mining at one time of shallow coal seams in China is mature, and its application is mainly concentrated in western mining areas, for example, the fully mechanized working face with large mining height of 1-2 coal seams in 12,401 working face of Shangwan Coal Mine in Shendong Mining Area (Xu et al., 2020; Yang and Liu 2020; Zhao et al., 2021), the buried depth of coal seams is 124–244 m, the thickness of coal seams is 7.56–10.97 m (average 9.26 m), and the Platts coefficient of coal seams is $f = 2 \sim 4$. However, for the coal seam with large buried depth, the coal seam bears the high static load of overlying strata. Under the disturbance of mining with full height mining at one time, roof instability and coal wall spalling will become more frequent. When coal and rock mass have impact tendency, the threat of dynamic disasters such as rock burst induced by overlying high static load superimposed with full height mining at one time disturbance is further increased (Dou et al., 2005; Xia et al., 2013; Liu et al., 2014; Pan 2019). At present, China is still in the trial stage for full height mining at one time with large buried depth, especially when the coal seam is soft, it is a challenge to successfully implement full height mining at one time.

In this paper, taking No. 3 coal seam of Lilou Coal Industry as the engineering background, the energy response mechanism of the roof is analyzed by establishing a cantilever beam model of the roof, the stored energy of the roof of different mining methods is compared, and the disturbed rock range of full height mining at one time and top caving mining is analyzed based on the field parameters. Furthermore, PFC^{2D} numerical software is used to simulate and analyze the instability process of roof and coal wall in full height mining at one time and top coal caving mining. By adjusting the *in-situ* stress value of the numerical model, the crack range of roof and coal wall is compared, and the buried depth of coal seam suitable for full height mining at one time is analyzed by inversion. Combined with the characteristics of on-site ground pressure behavior in No. 3 coal seam of Lilou Coal Industry, the adaptability of full height mining at one time in No. 3 coal seam of Lilou Coal Industry was determined, which provided a basis for selecting mining methods of coal seams under similar conditions.

2 CHARACTERISTICS OF STRATA BEHAVIOR IN WORKING FACE

The No. 1303 working face (Mining No. 3 Coal Seam) of Lilou Coal Industry is located in the middle and lower part of Shanxi

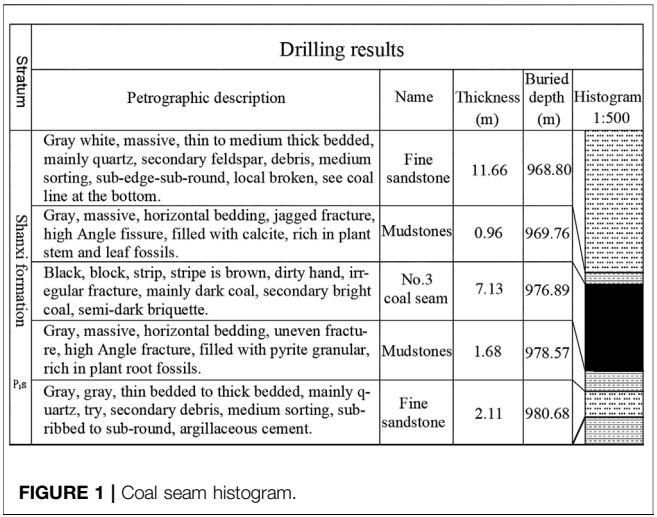

Stratum	Drilling results				
	Petrographic description	Name	Thickness (m)	Buried depth (m)	Histogram 1:500
Shanxi formation P_1s	Gray white, massive, thin to medium thick bedded, mainly quartz, secondary feldspar, debris, medium sorting, sub-edge-sub-round, local broken, see coal line at the bottom.	Fine sandstone	11.66	968.80	
	Gray, massive, horizontal bedding, jagged fracture, high Angle fissure, filled with calcite, rich in plant stem and leaf fossils.	Mudstones	0.96	969.76	
	Black, block, strip, stripe is brown, dirty hand, irregular fracture, mainly dark coal, secondary bright coal, semi-dark briquette.	No.3 coal seam	7.13	976.89	
	Gray, massive, horizontal bedding, uneven fracture, high Angle fracture, filled with pyrite granular, rich in plant root fossils.	Mudstones	1.68	978.57	
	Gray, gray, thin bedded to thick bedded, mainly quartz, try, secondary debris, medium sorting, sub-ribbed to sub-round, argillaceous cement.	Fine sandstone	2.11	980.68	

FIGURE 1 | Coal seam histogram.

formation, and the occurrence of coal seam (No. 3 Coal Seam) is mostly stable and its structure is relatively simple. The coal seam thickness is 6.70 ~ 7.31 m, the average coal thickness is 7.03 m, and the dip angle of coal seam is 4 ~ 16°, with an average of 13°. According to the field drilling histogram, the elevation of No. 3 coal floor in 1,303 working face is -994 ~ -890m, and the buried depth of coal seam is between 1,035 ~ 933 m. The immediate roof thickness of coal in working face 3 is 0.96 m, and the basic roof thickness is 8.12 m, the roof is mainly composed of medium and fine sandstone rock groups, with siltstone and mudstone rock groups locally. The immediate floor thickness of No.3 coal seam is 1.68 m, and the basic bottom thickness is 8.65 m, the floor is mainly composed of medium and fine sandstone rock groups, with siltstone mudstone rock groups locally. The coal seam histogram is shown in **Figure 1**. See **Table 1** for mechanical parameters of No.3 coal seam and roof and floor strata. From the mechanical parameters of coal seam No. 3 and roof and floor strata, it can be found that the strength of coal seam No. 3 is low, while the strength of roof and floor is high, which belongs to soft and thick coal seam.

Top coal caving mining is adopted in 1,303 working face of Lilou Coal Industry. In the process of mining, the hardness of the immediate roof strata is low, and the strength is weak. In the process of mining advancement, the caving increases with mining, and the basic roof periodic weighting rule is that the periodic weighting distance is between 20 and 22 m. During weighting, obvious weak vibration signals can be detected in the range of 0–150 m in front of the coal wall. After weighting, when the working face is advanced for 4–5 m, obvious spalling phenomenon occurs in the coal wall. Based on the above data, the analysis shows that the fracture span of the basic roof is 20–22 m, and the fracture position is about 4–5 m in front of the coal wall. When the working face is advanced for 4–5 m after the end of periodic weighting, the coal wall is at the fracture position, and the roof stress is concentrated on the coal wall at this time, which leads to the phenomenon of coal wall spalling. According to the appearance of on-site ore pressure, the schematic diagram of the pressure process is determined as shown in **Figure 2**. According to the appearance of on-site ore pressure, the schematic diagram of the pressure process is determined as shown in **Figure 2**. In the process of coal seam mining, the immediate roof caving along with mining, the basic roof forms a dynamic balance under the combined action of its own weight, overlying load and the supporting force of hydraulic support, and breaks and collapses in a cantilever beam structure.

3 COMPARISON ANALYSIS OF ENERGY RELEASE INTENSITY OF DIFFERENT MINING METHODS

3.1 Comparison Analysis of Bending Strain Energy of Basic Roof Rock Beam

The stress analysis of the basic roof in different mining methods is shown in **Figure 3**. The bending strain energy of the basic roof is analyzed by establishing a "cantilever beam" model, and the bending strain energy in the rock beam is compared between full height mining at one time and top coal caving mining. Under the condition of top coal caving mining, the top-coal is released, and the immediate roof fell as it was mined, so it is difficult for the top coal caving mining support to exert supporting force on the basic roof (Figure 3A), while under the condition of full height mining at one time, the support directly exerts stress on the direct top, and then can exert supporting force on the basic roof (Figure 3B). Under the action of self-weight stress and uniformly distributed load of overlying strata, the basic roof will undergo bending deformation, and when the tensile stress at the end of the rock beam reaches the tensile strength of the rock strata, the rock beam will break. therefore

$$R_t = \frac{M}{W} \tag{1}$$

TABLE 1 | Mechanical parameters of coal seam and roof and floor strata in 1,303 working face.

Items ground layer	Compressive strength σ_c (MPa)	Elastic modulus E (GPa)	Poisson's ratio μ	Tensile strength σ_t (MPa)	Cohesion c (MPa)	Friction angle φ (°)
Basic roof	103.99	21.65	0.24	7.15	29.97	34.30
Immediate roof	23.22	26.17	0.33	4.83	7.50	29.87
No.3 coal seam	14.65	1.33	0.22	0.59	0.56	38.89
Immediate floor	35.57	26.78	0.21	3.82	6.52	26.80
Basic bottom	128.12	32.81	0.24	8.31	26.04	37.60

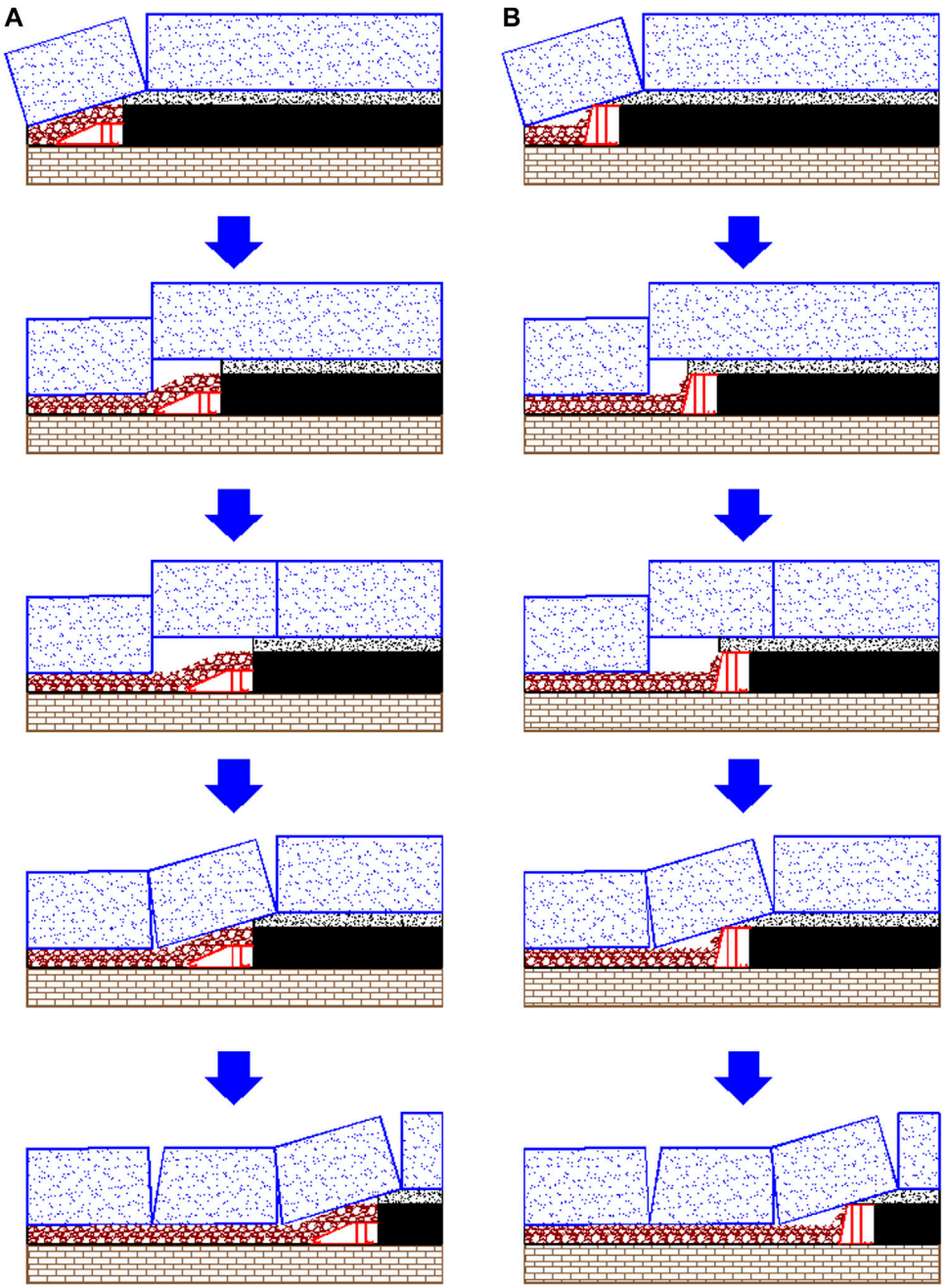

FIGURE 2 | Schematic diagram of periodic weighting process. **(A)** Top coal caving mining. **(B)** full height mining at one time.

In which: R_t -tensile strength of basic roof rock beam; M -bending moment of rock beam; W -bending stiffness of rock beam.

Contrasting the two mining methods, the bending stiffness W and tensile strength R_t of the basic roof are consistent, so the bending moment required for rock beam fracture under the two mining methods is consistent.

Under the condition of top coal caving mining:

$$M_T = \frac{1}{2}q_1 l_1^2 + \frac{1}{2}Ql_1 \tag{2}$$

In which: M_T- bending moment of rock beam under top coal caving mining condition; q_1- overburden load under top coal caving mining condition; l_1- Periodic weighting step under the condition of top coal caving mining; Q- Dead weight stress of fractured rock block.

Under the condition of full height mining at one time:

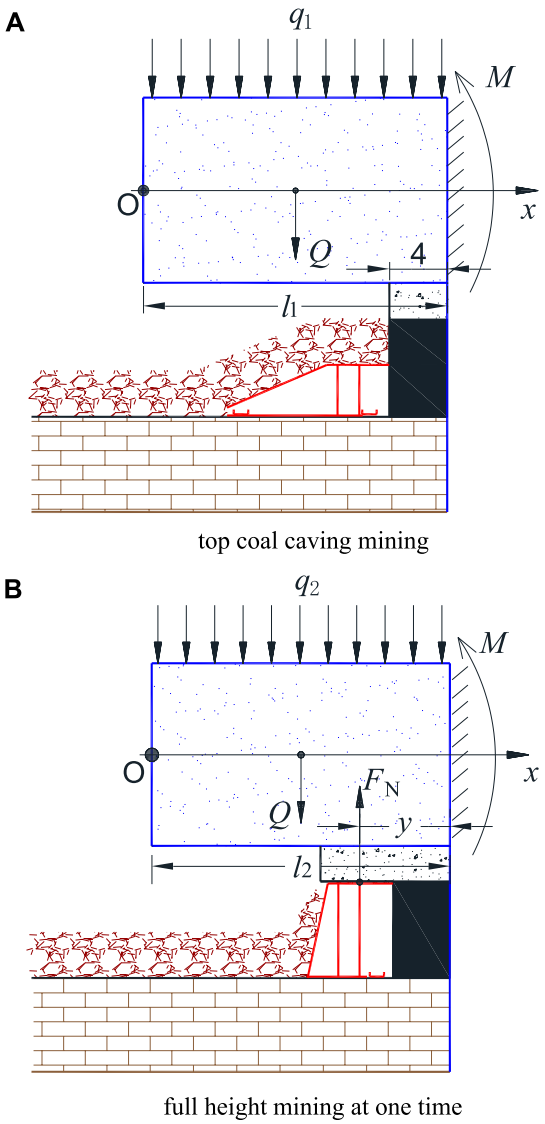

FIGURE 3 | Schematic diagram of stress on basic top rock beam. **(A)** top coal caving mining. **(B)** full height mining at one time.

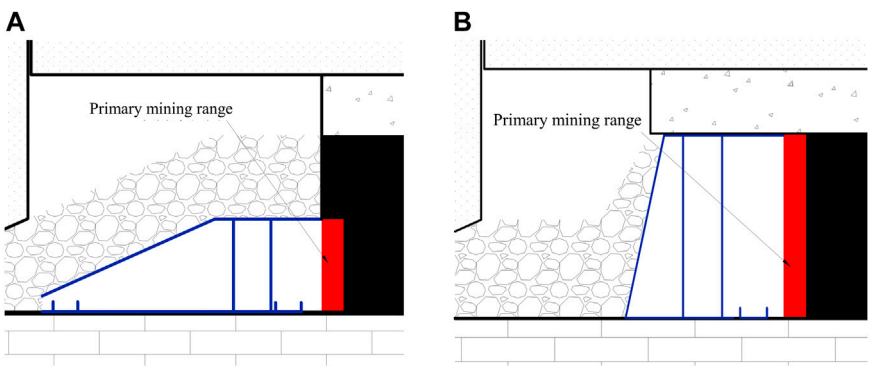

FIGURE 4 | Comparison of primary mining range of coal seam. **(A)** top coal caving mining. **(B)** full height mining at one time.

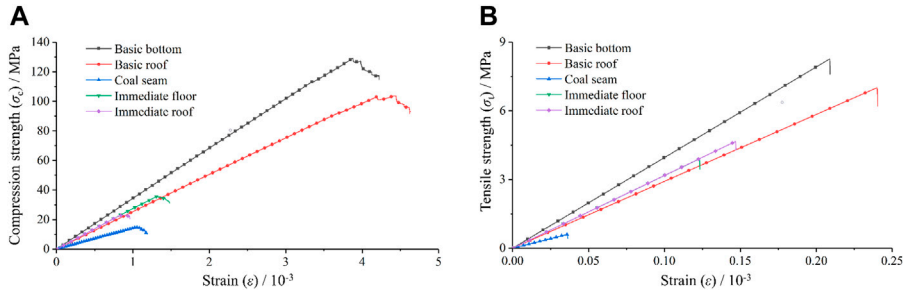

FIGURE 5 | Experimental results of various strata simulation. **(A)** Model compressive strength curve. **(B)** Model tensile strength curve.

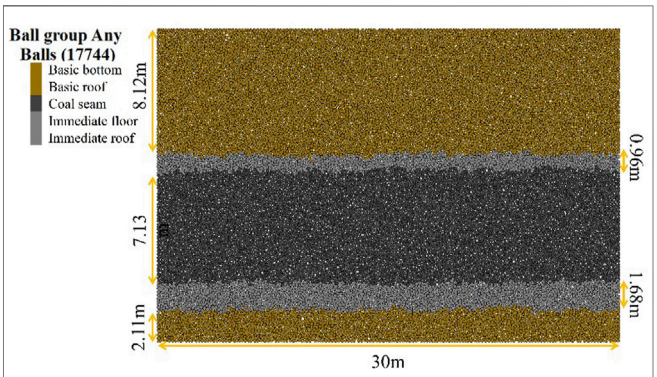

FIGURE 6 | Numerical model diagram of stope.

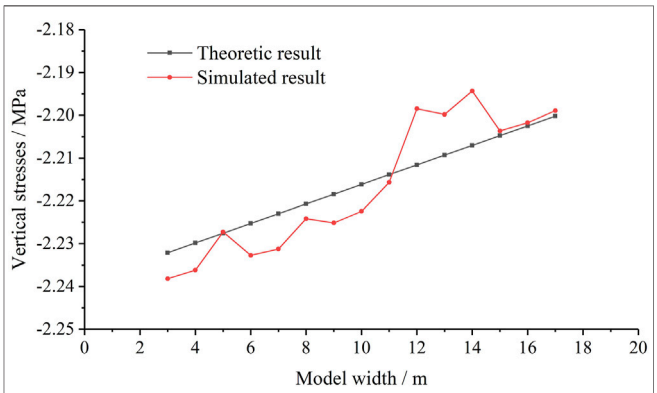

FIGURE 7 | Comparison of theoretical calculation and numerical simulation results of vertical stress.

$$M_F = \frac{1}{2}q_2 l_2^2 + \frac{1}{2}Ql_2 - F_N y \tag{3}$$

In which: M_F- bending moment of rock beam under the condition of full height mining at one time; q_2- overburden load under the condition of full height mining at one time; l_2- the periodic weighting step under the condition of full height mining at one time; y- the distance between the center of hydraulic support with full height mining at one time and the fracture position of roof rock beam, F_N- the supporting force of hydraulic support on the basic roof.

Due to the same bending moment required for rock beam fracture in the two mining methods, therefore

$M_T = M_F$then

$$\frac{1}{2}q_1 l_1^2 + \frac{1}{2}Ql_1 = \frac{1}{2}q_2 l_2^2 + \frac{1}{2}Ql_2 - F_N y \tag{4}$$

The coordinate system established in the basic top rock beam is shown in **Figure 3**. Before the basic roof breaks, the formula for calculating the bending strain energy in the rock beam is:

$$V_\varepsilon = \int_0^l \frac{M^2(x)}{2EI}dx \tag{5}$$

In which: V_ε- bending strain energy; E- elastic modulus; I- moment of inertia.

Calculation formula of bending strain energy under top coal caving mining condition is:

TABLE 2 | Input parameters of PFC^{2D} model for each rock stratum.

Ground layer	Surface gap g_s/mm	Effective modulus E^*/ GPa	Normal-to-shear stiffness ratio k^*	Tensile strength σt/ MPa	Cohesion c/ MPa	Density ρ/kg/m3
Basic roof	0.07	18.3	1.0	8.123	58.8	2,470
Immediate roof	0.07	19.9	1.0	5.4	10.56	2,340
Coal seam	0.07	1.05	1.0	0.7	8.0	1,350
Immediate floor	0.07	19.88	1.0	4.52	17.89	2,340
Basic bottom	0.07	24.8	1.0	9.58	72.4	2,470

TABLE 3 | Comparison between numerical simulation results and field mechanical parameters.

Ground layer	Numerical simulation results			Field mechanical parameter		
	Compressive strength σ_c/MPa	Elastic modulus *E*/GPa	Tensile strength σ_t/MPa	Compressive strength σ_c/MPa	Elastic modulus *E*/GPa	Tensile strength σ_t/MPa
Basic roof	103.77	21.91	7.01	103.99	21.65	7.15
Immediate roof	23.17	26.17	4.66	23.22	26.17	4.83
Coal seam	14.66	1.31	0.604	14.65	1.33	0.59
Immediate floor	35.69	26.93	39.03	35.57	26.78	3.82
Basic bottom	129.2	32.4	8.26	128.12	32.81	8.31

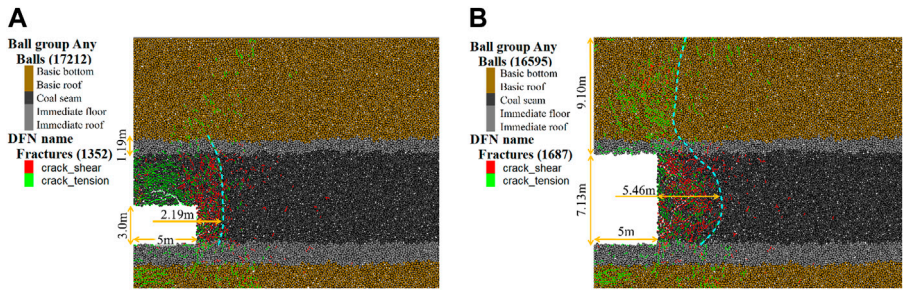

FIGURE 8 | Fracture propagation law of two mining methods. **(A)** Numerical simulation results of the top coal caving mining. **(B)** Numerical simulation results of the full height mining at one time.

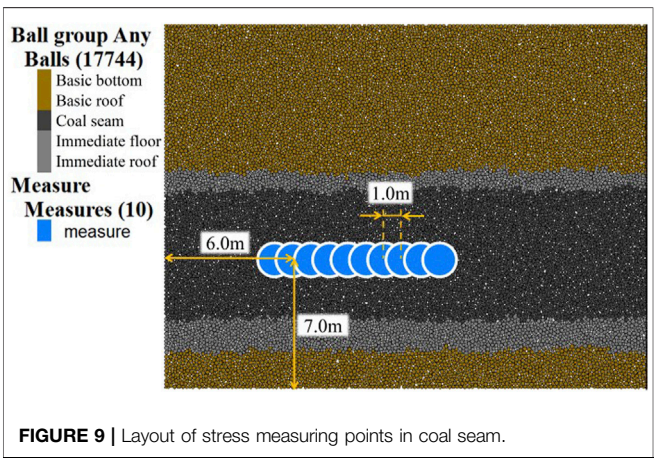

FIGURE 9 | Layout of stress measuring points in coal seam.

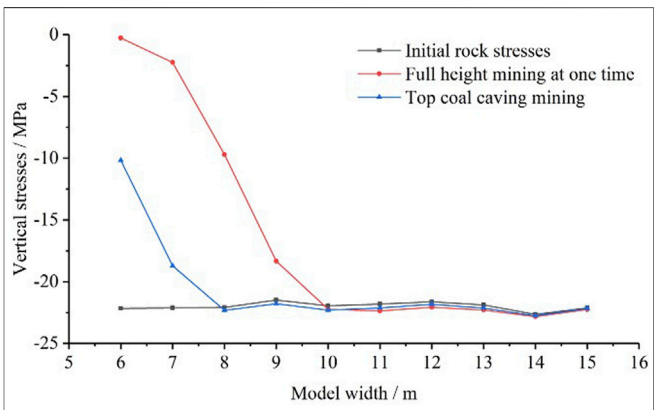

FIGURE 10 | Comparison of advanced stress after excavation.

$$V_{\varepsilon 1} = \int_0^{l_1} \frac{\left[q_1 x\left(\frac{x}{2}\right)\right]^2}{2EI} dx + \int_{\frac{l_1}{2}}^{l_1} \frac{\left[Q\left(x - \frac{l_1}{2}\right)\right]^2}{2EI} dx \quad (6)$$

In which: $V_{\varepsilon 1}$- bending strain energy of rock beam under top coal caving mining condition.

The formula for calculating bending strain energy under the condition of full height mining at one time is:

$$V_{\varepsilon 2} = \int_0^{l_2} \frac{\left[q_2 x\left(\frac{x}{2}\right)\right]^2}{2EI} dx + \int_{\frac{l_2}{2}}^{l_2} \frac{\left[Q\left(x - \frac{l_2}{2}\right)\right]}{2EI} dx \int_{l2-y}^{l_2} \frac{\{F_N[x - (l_2 - y)]\}^2}{2EI} dx \quad (7)$$

In which: $V_{\varepsilon 2}$- bending strain energy of rock beam under full height mining at one time condition.

Because the distance y between the center point of the hydraulic support with full height mining at one time and the fracture position of the roof rock beam is small, and the overlying immediate roof is soft and broken, the work done by the hydraulic support with full height mining at one time on the basic roof is mainly absorbed by the broken rock layer of the immediate roof, the supporting force of the hydraulic support will not displace in the basic roof, so the work done by the hydraulic support on the basic roof can be ignored, that is, **Eq. 7** can be simplified as follows:

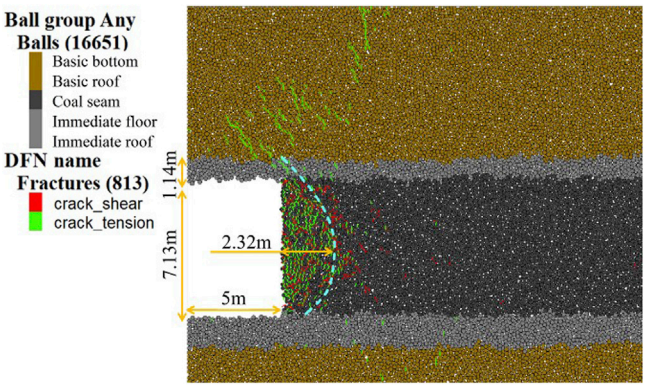

FIGURE 11 | Fracture propagation form of full height mining at one time after stress debugging.

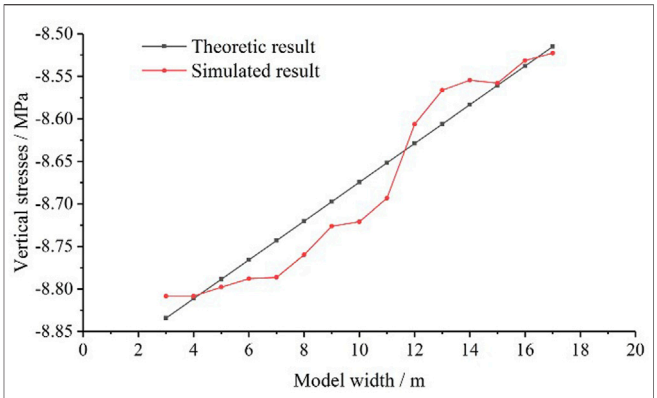

FIGURE 12 | Comparison of debugging stress debugging results of full height mining at one time.

$$V_{\varepsilon 2} = \int_0^{l_2} \frac{\left[q_2 x\left(\frac{x}{2}\right)\right]^2}{2EI} dx + \int_{\frac{l_2}{2}}^{l_2} \frac{\left[Q\left(x - \frac{l_2}{2}\right)\right]^2}{2EI} dx \tag{8}$$

According to the calculation **Eq. 4**, when the weighting steps of the two mining methods are the same ($l_1 = l_2$), then $q_2 > q_1$; When the overburden load of the two mining methods is the same ($q_1 = q_2$), then $l_2 > l_1$.

Because $q_2 > q_1$ or $l_2 > l_1$, substituting into **formulas (6)** and **(8)**, the bending strain energy stored in the basic roof rock layer is $V_{\varepsilon 2} > V_{\varepsilon 1}$, that is, the energy released when the basic roof breaks in full height mining at one time is greater than that in top coal caving mining.

3.2 Comparative Analysis of Mining Disturbance Range

In the process of top coal caving mining, the range of mining is small, the range of rock disturbed by primary mining is relatively small, and the primary release strength of bending strain energy stored in disturbed rock is relatively small. However, in the process of full height mining at one time, the range of mining is large, the rock strata disturbed by mining is relatively large, and the bending strain energy stored in the disturbed rock strata has relatively large one-time release strength. The primary mining range of different mining methods is shown in **Figure 4**.

At the same time, when the mining disturbance is large and there is more energy released at one time (for example, periodic weighting), the top coal in top coal caving mining is low in strength and easy to break, which can play a good role in energy absorption and buffering (Wang 2007). However, there is no coal seam buffer layer when the full height mining at one time, and the energy released at one time will directly act on the hydraulic support and coal wall when the roof breaks, further increasing the risk of coal wall spalling.

4 COAL WALL STABILITY COMPARATIVE ANALYSIS

4.1 Calibration of Meso-parameters of Numerical Model

In order to compare the stability of coal wall between the two mining methods, numerical simulation is used for analysis. Considering the advantages of PFC software in fracture propagation simulation, this paper chooses PFC software for simulation analysis. See **Table 1** for mechanical parameters of coal seam and roof and floor strata in Lilou Coal Industry. Because there is a certain difference between the input parameters and the output parameters in the numerical model, before the simulation analysis, first check the input parameters of the rock strata (Chen et al., 2018; Feng 2020).

A standard block of 100 × 50 mm is established, the model contains 1,481 particles, and the Flat-joint contact model is adopted among the particles, which mainly checks the uniaxial compressive strength σ_c, elastic modulus E and tensile strength σ_t of the rock strata. By debugging the particle surface gap, effective modulus, normal-to-shear stiffness ratio, tensile strength, cohesion and particle density in the numerical model, the mechanical parameters of the numerical model correspond to the laboratory experimental values, and the input parameters in the numerical model of each rock strata are determined as shown in **Table 2**. The simulation results of uniaxial compressive strength and tensile strength of each rock strata are shown in **Figure 5**. See **Table 3** for comparison of simulation results of various rock parameters with field mechanical parameters. from **Table 3**, it can be seen that numerical simulation results of compressive strength, elastic modulus and tensile strength of test block are close to field mechanical parameters, so all parameters can be used for subsequent simulation of coal seam excavation.

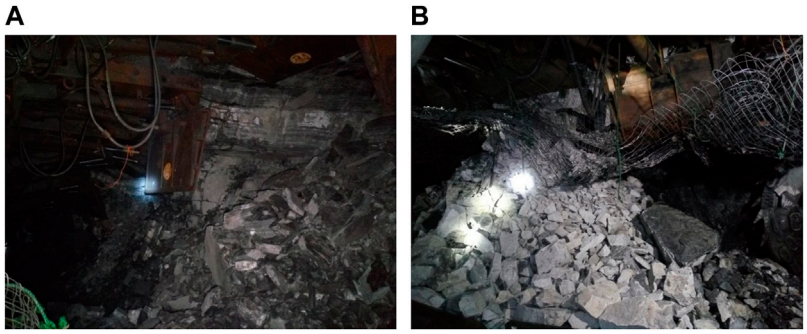

FIGURE 13 | Status of 103 fully mechanized top coal caving face. **(A)** Serious coal spalling. **(B)** Roof crushing and gangue leakage.

4.2 Establishment of Numerical Model

In order to prominent the failure process of surrounding rock and stress evolution law of coal seam after coal seam excavation, the model stope should be as large as possible, and the model should be as small as possible on the basis of eliminating boundary effect. After repeated debugging, the model height should be 20 m and the model strike length should be 30 m. According to geological histogram **Figure 1**, the thickness of each rock strata included in the model is determined as follows: basic roof 8.12 m, immediate roof 0.96m, coal seam 7.13 m, immediate floor 1.68 m and basic bottom 2.11 m. The model contains 17,744 particles. See **Table 3** for various parameters of coal strata, and the established model is shown in **Figure 6**.

4.3 Debugging of Stress Applied by Numerical Model

The basic roof buried depth is 960.68 m, the average density of overlying fine sandstone and mudstone is 2280 kg/m^3, and the gravity acceleration is 10 m/s^2. It is calculated that the stress on the upper surface of the model is about 21.89MPa, and the stress increases by 0.0228 MPa for every 1 m increase in depth. In the middle of the trend of the numerical model, vertical stress measuring points are set from the bottom of the model to the top of the model within 3–17 m, and the evolution law of vertical stress in the middle of the model is monitored. Repeated debugging confirms that 3.66×10^5 N downward pressure is applied in the upper part of the model within 18–20 m, while 2×10^3 N downward uniform pressure (simulated stress gradient) is applied in the upper part of the model within 0–20 m. The comparison between theoretical estimation results ($\sigma = \gamma h$) and simulated results is shown in **Figure 7**. The overall trend of the two results is close, but the stress in the simulated results fluctuates. The reason for the fluctuation is that the rock density is selected according to the average value in the theoretical calculation, while different rock layers are calculated according to different densities in the simulated results. In summary, it can be seen that the modeling method, parameter selection and external force applied of the numerical model are reasonable, which can be used for subsequent analysis.

4.4 Analysis of Numerical Simulation Results

4.4.1 Analysis of Failure State of Coal Wall and Roof Strata

Coal seam excavation starts from the left side of the model, referring to the field stope range, which is 5 m. In the process of mining, the coal seam mining height is 3.0 m when the top coal caving mining is carried out, and the coal body of 7.13 m is fully extracted when the full height mining at one time. PFC5.0 software automatically determines the running timestep of the model as 1 according to the contact stiff-ness and particle size between particles, and stops running when cracks in the roof of the numerical simulation model are through. In the process of simulation, it was found that the roof cracks were firstly connected when the full height mining at one time numerical simulation model ran 430 timesteps, so the two numerical simulation models stopped after running 430 timesteps. **Figure 8** shows the fracture propagation patterns obtained by simulating two mining methods.

It can be seen from Figure 8A that during top coal caving mining, under the action of initial rock stress and mining disturbance stress, cracks occur in the coal body, and the cracks form obvious up-and-down through cracks at 2.19 m in front of the coal wall, which extend to 1.19 m above the coal seam, and the integrity of the basic roof strata upward is good, with only a few micro cracks. It can be seen from Figure 8B that the cracks in the coal body form obvious up-and-down through cracks at 5.46 m in front of the coal wall, which extend to the top of the model, and the basic roof is fractured and damaged. the cracks range of coal wall under the condition of full height mining at one time is much larger than that during top coal caving mining, and the damage depth of coal wall during full height mining at one time is 2.5 times of that during top coal caving mining, and the phenomenon of coal wall spalling is serious.

4.4.2 Comparison of Stress in Coal Seam After Excavation

In order to compare the evolution law of coal advanced stress during top coal caving mining and full height mining at one time, 10 stress measuring points are arranged at an interval of 1.0 m at a distance of 7 m from the bottom of the model (at a height of 3.2 m in coal seam). The radius of measuring point is 1m, and from left

to right, measuring point 1 is located 6 m away from the leftmost side of the model (the left edge of measuring point 1 is located at the coal wall), and the layout of measuring points is shown in **Figure 9**. The comparison of advanced stress after excavation is shown in **Figure 10**.

It can be seen from **Figure 10** that stress reduction occurs near the coal wall after top coal caving mining and full height mining at one time. After full height mining at one time, under the action of overburden load and excavation disturbance load, the coal wall collapses and loses its bearing capacity. The vertical stress obtained by monitoring the coal wall position is 0.27 MPa. With the increase of the distance from the coal wall, the coal stress gradually recovers, and the coal stress is restored to the original at 5 m from the coal wall (about 10 m from the leftmost side of the model). After top coal caving mining, the vertical stress obtained by monitoring the coal wall position is about 10.2 MPa, so the coal wall has not completely lost its bearing capacity at this time, that is, the coal wall has not collapsed, and the coal stress has returned to the original rock stress level at 3 m away from the coal wall (about 8 m away from the leftmost side of the model). It can be seen that the damage degree of coal wall in top coal caving mining is far less than that in full height mining at one time. When full height mining at one time occurs, the coal wall collapses, and the stress of coal body is basically reduced to 0. However, although a large number of cracks are developed in the coal wall during top coal caving mining, the bearing capacity is not lost, that is, the coal wall does not collapse. Combined with the law of crack propagation, it is further verified that the stability of coal wall is poor when the full height mining at one time under this large buried depth condition, which is not conducive to on-site safety production.

4.5 Adaptability Analysis of Full Height Mining at One Time

In order to study the adaptability of the full height mining at one time, reduce the overlying load of the numerical model, and the microscopic parameters and running time of rock particles are kept unchanged, so as to realize that the cracks range of coal seam and roof at the full height mining at one time after stress debugging is similar to the damage result of full height mining at one time under the original rock stress condition, the coal seam depth at the full height mining at one time is applicable under this coal seam strength through stress inversion analysis. After debugging, the model applies a downward pressure of 1.4×10^5 N in the range of 18–20 m and a downward uniform pressure of 500N in the range of 0–20 m, and obtains the rock strata failure range when the full height mining at one time, as shown in **Figure 11**. At this time, the maximum failure depth of coal reaches 2.32 m in front of the coal wall, and the through fracture inside the coal body extends to 1.14 m above the coal seam, which is close to the fracture expansion when the top coal caving mining under the initial rock stress condition.

The vertical stress in the middle position of the monitored model strike is shown in **Figure 12**. By comparison, it is found that the theoretical value of overlying load of coal seam is about 8.65 MPa, and the corresponding burial depth at this time is about 380 m (the average density of overlying strata is 2280 kg/m^3, and the gravity acceleration is 10 m/s^2, $h = \sigma/\gamma$). Under this coal seam strength condition, when the buried depth of coal seam is less than 380m, the stability of coal wall and roof strata can be ensured by adopting full height mining at one time.

4.6 Field Application Analysis

In the process of site mining, the 1,303 fully mechanized caving face has a mining height of 3.0 m and a coal drawing height of 4.13 m. In the middle of the face, ZF15000/23/42 top coal caving hydraulic support and ZFG15000/25/42H top coal caving transition hydraulic support are used for support. Although top coal caving mining is adopted in 1,303 working face, the phenomenon of coal wall splints is still serious in the mining process, with severe ore pressure, poor stability of coal wall, and serious breakage and leakage of gangue in roof, as shown in **Figure 13**Figure 13A and Figure 13B. At the same time, weak vibration events often occur in the working face, which affects the working face advance speed and production efficiency. It can be seen that it is still difficult to maintain the stability of roof and coal wall in 1,303 working face caving coal mining, and further it can be seen that full height mining at one time is not suitable.

5 THE CONCLUSION

1) By establishing the mechanical model of the basic roof "cantilever beam" for comparative analysis of bending strain energy, it is determined that the energy released when the basic roof breaks is greater than that of the top coal caving mining. Further comparison shows that the rock strata disturbed by the first mining is relatively small in the top coal caving mining, and the energy release intensity of disturbed rock strata is relatively small.
2) It is found that through cracks appear in the roof of simulated full height mining at one time, the coal wall failure depth reaches 5.46 m, and the coal wall collapses and loses its bearing capacity. During top coal caving mining, the roof crack extends to 1.19 m above the coal seam, and the coal wall failure depth is 2.19 mm. The coal wall can still exert part of its bearing capacity, and its bearing stress is 10.2 MPa.
3) In order to study the adaptability of the full height mining at one time in the field, by reducing the overlying load of numerical simulation model, make the development degree of full height mining at one time coal seam and roof crack after coal seam excavation match with top coal caving mining. By comparing the simulated vertical stress with the theoretical stress, it is determined that the full height mining at one time is reliable when the buried depth is less than 380 m.

DATA AVAILABILITY STATEMENT

The raw data supporting the conclusion of this article will be made available by the authors, without undue reservation.

AUTHOR CONTRIBUTIONS

QL provided ideas and theoretical analysis for the paper. YJ and XZ provided field data for the paper. HW, KL and ZW conducted numerical simulation and data analysis. All members participate in writing articles.

FUNDING

The research is supported by the key project of natural science foundation of Shandong province (Grant Numbers ZR2020KE030). Supported by NSFC Youth Fund (Grant Numbers 52104136). The field information from the study site was provided by the Lilou Coal Mine.

ACKNOWLEDGMENTS

The author expresses his gratitude for this support.

REFERENCES

Chen, P. Y., Kong, Y., and Yu, H. M. (2018). Research on the Calibration Method of Microparameters of a Uniaxial Compression PFC^{2D} Model for Rock. *Chin. J. Undergr. Space Eng.* 14 (05), 1240–1249.

Dou, L. M., Lu, C. P., Mou, Z. L., Qin, Y. H., and Yao, J. M. (2005). Intensity Weakening Theory for Rockburst and its Application. *J. China Coal Soc.* (06), 690–694. doi:10.3321/j.issn:0253-9993.2005.06.003

Feng, K. W. (2020). Research on Calibration of Micro Parameters of PFC^{2D} Model in Uniaxial Compression of Coal Similar Materials. *Saf. Coal Mines* 51 (04), 5–9.

Feng, L. F., Dou, L. M., Wang, X. D., Jin, D. W., Cai, W., Xu, G. G., et al. (2019). Mechanism of Mining Advance Speed on Energy Release from Hard Roof Movement. *J. China Coal Soc.* 44 (11), 3329–3339. doi:10.13225/j.cnki.jccs.2018.1671

Gong, P. L., and Jin, Z. M. (2008). Mechanical Model Study on Roof Control for Fully-Mechanized Coalface with Large Mining Height. *Chin. J. Rock Mech. Eng.* 2008 (01), 193–198. doi:10.3321/j.issn:1000-6915.2008.01.027

Hao, H. J., Wu, J., Zhang, Y., and Yuan, Z. B. (2004). The Balance Structure of Main Roof and its Action to Immediate Roof in Large Cutting Height Workface. *J. China Coal Soc.* (02), 137–141. doi:10.3321/j.issn:0253-9993.2004.02.003

He, X., Zhao, Y., Yang, K., Zhang, C, and Han, P (2021). Development and Formation of Ground Fissures Induced by an Ultra Large Mining Height Longwall Panel in Shendong Mining Area[J]. *Bull. Eng. Geol. Environ.* (9), 2021. doi:10.1007/s10064-021-02429-6

Hu, G. W., and Jin, Z. M. (2006). Study on Mining Pressure Observation and its Developing Law of Fully Mechanized Mining Face with Large Mining Height. *J. Taiyuan Univ. Technol.* (02), 127–130.

Hu, S. X., Ma, L. Q., Guo, J. S., and Yang, P. J. (2018). Support-surrounding Rock Relationship and Top-Coal Movement Laws in Large Dip Angle Fully-Mechanized Caving Face. *J] Int. J. Min. Sci. And Technol.* 28 (3), 533–539. doi:10.1016/j.ijmst.2017.10.001

Hubbret, M. K., and Wills, D. G. (1957). Mechanics of Hydraulic Fracturing[J]. *Transcations Soc. Petroleum Eng. AIME* 210, 153–168.

Ju, J. F., Xu, J. L., and Zhu, W. B. (2014). Influence of Key Strata Cantilever Structure Motion on End-Face Fall in Fully-Mechanized Face with Super Great Mining Height. *J. China Coal Soc.* 39 (07), 1197–1204. doi:10.13225/j.cnki.jccs.2013.1000

Ju, J. F., Xu, J. L., Zhu, W. B., Wang, Q. X., and Hao, X. J. (2012). Strata Behavior of Fully-Mechanized Face with 7.0 M Height Support. *J. Min. Saf. Eng.* 29 (03), 344–350+356.

Ju, J., and Xu, J. (2013). Structural Characteristics of Key Strata and Strata Behaviour of a Fully Mechanized Longwall Face with 7.0m Height Chocks. *Int. J. Rock Mech. Min. Sci.* 58, 46–54. doi:10.1016/j.ijrmms.2012.09.006

Kong, D. Z., Pu, S. J., Zheng, S. S., Wang, C. H., and Lou, Y. H. (2019). Roof Broken Characteristics and Overburden Migration Law of Upper Seam in Upward Mining of Close Seam Group[J]. *Geotechnical Geol. Eng.* 2019 (4). doi:10.1007/s10706-019-00836-x

Liang, Y. P., Li, B., Yuan, Y., Zou, Q. L., and Jia, L. X. (2017). Moving Type of Key Strata and its Influence on Ground Pressure in Fully Mechanized Mining Face with Large Mining Height. *J. China Coal Soc.* 42 (06), 1380–1391. doi:10.13225/j.cnki.jccs.2016.1320

Liang, Y. P., Li, B., and Zou, Q. L. (2019). Movement Type of the First Subordinate Key Stratum and its Influence on Strata Behavior in the Fully Mechanized Face with Large Mining Height. J]*Arabian J. Geosciences* 12 (2). doi:10.1007/s12517-018-4208-9

Liu, S. H., Mao, D. B., Qi, Q. X., and Li, F. M. (2014). Under Static Loading Stress Wave Propagation Mechanism and Energy Dissipation in Compound Coal-Rock. *J. China Coal Soc.* 39 (S1), 15–22. doi:10.13225/j.cnki.jccs.2013.0411

Ning, Y. (2009). Mechanism and Control Technique of the Rib Spalling in Fully Mechanized Mining Face with Great Mining Height. *J. China Coal Soc.* 34 (01), 50–52.

Pan, J. F. (2019). Theory of Rockburst Start-Up and its Complete Technology System. *J. China Coal Soc.* 44 (1), 173–182.

Wang, G. F., and Pang, Y. H. (2018). Full-mechanized Coal Mining and Caving Mining Method Evaluation and Key Technology for Thick Coal Seam. *J. China Coal Soc.* 43 (01), 33–42. doi:10.13225/j.cnki.jccs.2017.4200

Wang, H., Liu, Y., Tang, Y., Gong, H., and Xu, G. (2021). Failure Mechanisms and the Control of a Longwall Face with a Large Mining Height within a Shallow-Buried Coal Seam. *Shock Vib.* 2021 (7), 1–11. doi:10.1155/2021/8494913

Wang, J. C. (2007). Mechanism of the Rib Spaling and the Controlling in the Very Soft Coal Seam. *J. China Coal Soc.* 155 (8), 785–788. doi:10.3321/j.issn:0253-9993.2007.08.001

Wong, R. H. C., and Wang, S. W. (2002). "Experimental and Numerical Study on the Effect of Material Property, Normal Stress and the Position of Joint on the Progressive Failure under Direct Shear[A]," in *Narms-tac2002, Mining and Tunneling Innovation and Opportunity[C* (Toronto, 1009–1016.*]*

Xia, Y. X., Lan, H., and Mao, D. B. (2013). Rock-burst Start Conditions and Prevention Technology under Static and Dynamic Load Action. *J. Min. And Strata Control Eng.* 18 (05), 83–86.

Xu, H. Z., Li, Q. S., Li, X. B., Zhang, G. J., Yang, Y. L., He, W. R., et al. (2020). Structural Evolution of Overburden and Surface Damage Caused by High-Intensity Mining with Shallow Depth. *J. China Coal Soc.* 45 (08), 2728–2739.

Xu, J. L., and Ju, J. F. (2011). Structural Morphology of Key Stratum and its Influence on Strata Behaviors in Fully-Mechanized Face with Supper-Later with Supper-Large Mining Height. *Chin. J. Rock Mech. Eng.* 30 (08), 1547–1556.

Yang, J. Z., and Liu, Q. J. (2020). Analysis and Measured of Strata Behavior Law and Mechanism of 8.8 Multra-High Mining Height Working Face. *Coal Sci. Technol.* 45 (08), 2728–2739.

Yang, J. Z., Zhang, K. G., Wang, Z. R., and Pang, N. Y. (2020). Technology of Weakening and Danger-Breaking Dynamic Disasters by Hard Roof. *J. China Coal Soc.* 45 (10), 3371–3379. doi:10.13225/j.cnki.jccs.2020.0599

Zhang, C., Zhao, Y., He, X., Guo, J, and Yan, Y (2020). Space-sky-surface Integrated Monitoring System for Overburden Migration Regularity in Shallow-Buried High-Intensity Mining[J]. *Bull. Eng. Geol. Environ.*, 1–15. doi:10.1007/s10064-020-02026-z

Zhang, C. W., Jin, Z. X., Song, X. M., Feng, G. R., Li, Z., Gao, R., et al.(2020) Failure Mechanism and Fracture Aperture Characteristics of Hard Thick Main Roof

Based on Voussoir Beam Structure in Longwall Coal Mining[J]*Energy Sci. Eng.*; 2020, 8(2)doi:10.1002/ese3.492

Zhang, G. Q., and Chen, M. (2010). Dynamic Fracture Propagation in Hydraulic Refracturing[J]. *J. Petroleum Sci. Eng.* (70), 266–272. doi:10.1016/j.petrol.2009.11.019

Zhang, N. B., Liu, C. Y., and Yang, P. J. (2016). Flow of Top Coal and Roof Rock and Loss of Top Coal in Fully Mechanized Top Coal Caving Mining of Extra Thick Coal Seams. *[J] Arabian J. Geosciences* 9 (6). doi:10.1007/s12517-016-2493-8

Zhao, Y. X., Ling, C. W., Liu, B., and He, X. (2021). Fracture Evolution and Energy Dissipation of Overlying Strata in Shallow-Buried Underground Mining with Ultra-high Working Face. *J. Min. Saf. Eng.* 38 (01), 9–30. doi:10.13545/j.cnki.jmse.2020.0212

Conflict of Interest: XZ and YJ was employed by the company Shandong Lilou Coal Industry Co., Ltd.

The remaining authors declare that the research was conducted in the absence of any commercial or financial relationships that could be construed as a potential conflict of interest.

Publisher's Note: All claims expressed in this article are solely those of the authors and do not necessarily represent those of their affiliated organizations, or those of the publisher, the editors and the reviewers. Any product that may be evaluated in this article, or claim that may be made by its manufacturer, is not guaranteed or endorsed by the publisher.